Fracture Toughness Characterizations of Compatibilized Polyamide-6 (PA6)/ Poly(phenylene ether) (PPE) Blends

Kuo-Chan Chiou[1], Feng-Chih Chang[1,*] and Yiu-Wing Mai[2]

1. *Institute of Applied Chemistry, National Chiao-Tung University, Hsinchu 30050, Taiwan*
2. *Centre for Advanced Materials Technology, Department of Mechanical and Mechatronic Engineering, University of Sydney, Sydney, N.S.W., Australia*

Received October 3, 2000; revised October 31, 2000; accepted November 17, 2000

Abstract: Under the plane-strain condition, the material properties, K_{IC} and G_{IC}, of the blends, brittle or with small-scale yielding, increase with increasing elastomer content. To evaluate the critical J-integral for the ductile blends, several methods have been compared to understand the influence of elastomer content and different thicknesses using single-edge notch-bend specimens. For a given thickness, the fracture toughness increases with increasing elastomer content. Moveover, the slope of the R-curve becomes gradually steeper with increasing elastomer content and decreasing specimen thickness. J_{IC} values determined from ASTM E813-89 and modified ASTM E813-81 methods always give the highest and the lowest values, respectively. J_{IC} values determined from three other methods are comparable and can be employed to characterize the fracture toughness of the compatibilized PA6/PPE blends. It is noted that J_{IC} values determined from the modified ASTM E813-89 and the hysteresis energy methods are apparently independent of thickness. Therefore, these two methods may be considered as potential alternative techniques to evaluate the critical J-integral for toughened polymer blends.

Keywords: PA6, PPE, Compatibilization, Polymer blends, J-integral.

Introduction

As polymeric materials have been utilized extensively in load-bearing applications, it is necessary to have a thorough understanding of their ability to resist fracture. For brittle materials, linear elastic fracture mechanics (LEFM) has been widely used to characterize their fracture behavior. The geometric and size-independent parameters, K_{IC} and G_{IC}, have been employed to represent the true material properties for most glassy polymers and polymer blends, provided that certain restrictive size criteria of the tested specimen have been met. These conditions are set to satisfy the requirements of plane-strain fracture behavior so that the developed plastic zone in the vicinity of the crack tip is small compared to the specimen dimensions. Hence, the energy dissipation is locally limited to the crack tip region and the fracture behavior can be described from the energy change in an elastic analysis.

To increase the fracture toughness of polymers and polymer blends, rubbers are often added [1]. However, LEFM cannot usually be applied to these toughened polymers due to their low yield strength, and the size requirement may be beyond the range of thickness which can be practically produced with standard processing conditions. Their fracture behavior occurs in the elastic-plastic region. To overcome this difficulty, Rice [2] proposed the J-integral concept to characterize the stress-strain singularity at a crack tip in an elastic or elastic-plastic material. Begley and Landes [3,4] then made use of the J-integral concept to develop a measurement method for the fracture toughness, J_{IC}, which represents the energy required to initiate crack growth. This J-integral method has been extensively and suc-

*To whom all correspondence should be addressed.
Tel: 886-3-5712121 ext. 56502; Fax: 886-3-5723764
E-mail: changfc@cc.nctu.edu.tw

J. Polym. Res. is covered in ISI (CD, D, MS, Q, RC, S), CA, EI, and Polymer Contents.

cessfully used to characterize various ductile polymeric materials [5-19] by the multiple-specimen method developed by Begley and Landes or the single-specimen method developed by Rice et al. [20]. A critical J integral, J_{IC}, is commonly used to characterize the fracture toughness of a ductile material with large-scale yielding. The procedure for J_{IC} determination has been standardized by ASTM E813 methods [21,22] for metallic materials and extended to various toughened polymers and polymer blends. However, the optimum testing procedure for polymeric materials has not yet been conclusively and unambiguously established. Therefore, several different approaches for J_{IC} evaluation have been proposed [16,19, 23-30].

From our previous study [31], this elastomer-modified PA6/PPE/SMA blends in the Izod impact tests could be partitioned into three categories : brittle, semi-ductile and ductile materials. There was a critical elastomer content, ~15 phr, for the ductile-brittle transition of the PA6/PPE/SMA blends. In this study, the brittle blend fracture behavior obeys LEFM and its toughness can be properly described by K_{IC} and G_{IC}. The ductile blend's fracture toughness is characterized by two key ASTM standard methods the (ASTM E813-81 and 89 method), their modified methods and a non-conventional hysteresis energy method. Under the same size criteria, comparison its carried out to understand the differences between these methods. Moreover, the effect of specimen thickness on fracture toughness of PA6/PPE/SMA blends is investigated.

Experimental

1. Materials

All materials were supplied from various commercial sources. Polyamide-6 (PA6), trademark 1010C2, with a relative viscosity of 2.3, was obtained from Mitsubishi Kasei Co. Ltd., Japan. Poly(phenylene ether) (PPE), trademark HPP-820, with an intrinsic viscosity of 0.4 dL/g was supplied by General Electrical Co., USA. The reactive compatibilizer, poly(styrene-*co*-maleic anhydride) (SMA), trademark Dylark 232, with 8% MA and $M_W = 2 \times 10^5$, was supplied by Arco Chemical Co., USA. The elastomer, G1651, with a styrene end-block, was produced by Shell Chemical Co., USA.

2. Samples preparation

All blends were prepared on a co-rotating 30 mm twin-screw extruder (L/D = 36, Sino-Alloy Machinery Inc.) with a rotational speed of 250 rpm. The barrel temperatures were pre-set and varied from 210 to 290 °C. Standard tensile and single-edge notch-bend (SENB) specimens with different thickness(t) (4, 6, 8 and 10 mm) were prepared with an Arburg 3 oz injection molding machine. The dimension of a SENB specimen was 90 × 20 × t mm. The temperature for injection molding varied from 280 to 295 °C.

3. Characterization

Standard tensile tests (ASTM D638) were carried out at a cross-head speed of 2 mm/min. Fracture toughness tests were conducted on SENB specimens at the same speed according to ASTM D5045 for K_{IC} and G_{IC} and the standardized and modified ASTM E813 for J_{IC}. The unconventional hysteresis energy procedure was also carried out on the same SENB specimens that were loaded to a pre-determined displacement at a cross-head rate of 2 mm/min and then unloaded at the same rate. A notch was introduced on the mid-length of one side of a SENB specimen using a guillotine-like apparatus with a fresh razor blade driven by a screw with 1 mm pitch. A sharp precrack was made to meet the recommended ratio of thickness to depth, 0.5. To avoid possible plastic deformation at the crack tip, the razor blade should be always fresh and the pushing speed as slow as practical. This procedure was carried out on six specimens to obtain the average properties based upon every standard or modified testing method utilized in this study.

Background of Theory

1. ASTM D5045 standard method

K_{IC} determined by this method characterizes the resistance of a material to fracture with the presence of a sharp crack under severe tensile constraint. Such a stress state near the crack front approaches plane-strain and the plastic zone is small compared with the crack size and the specimen dimensions. K_{IC} is the lowest limiting value of fracture toughness. For SENB specimen, K_Q, the conditional K_{IC}, can be expressed by (S/W = 4):

$$K_Q = \left(\frac{P_Q}{BW^{1/2}} \right) f(x) \tag{1}$$

where $(0 < x = a/W < 1)$

$$f(x) = 6x^{1/2} \left[\frac{1.99 - x(1-x)(2.15 - 3.93x + 2.7x^2)}{(1+2x)(1-x)^{3/2}} \right] \tag{2}$$

where P_Q is the conditional load, B is the specimen thickness, S is the span, W is the specimen depth and a is the crack length.

For plane-strain linear elastic fractures, K_{IC} is related to the critical strain energy release rate, G_{IC}, by:

$$G_{IC} = \frac{K_{IC}^2}{E}(1-\nu^2) \tag{3}$$

where E is elastic modulus and ν is Poisson's ratio.

2. KIC validity requirements

To obtain a valid K_{IC} value, a specimen must meet certain size requirements to achieve plane-strain fracture. According to ASTM D5045, these requirements are :

$$0.45 < a/W < 0.55 \tag{4}$$

$$B,\ a,\ (W-a) > 2.5\ (K_Q/\sigma_y)^2 \tag{5}$$

$$P_{max}/P_Q < 1.1 \tag{6}$$

where σ_y is the yield stress of the tested material.

3. J-integral

For small-scale yielding, the J-integral is equal to the strain energy release rate, G, which in theory is related to the stress intensity factor, K. The J-integral is defined by :

$$J = \int_{\Gamma} \left(\overline{W}\,dy - \overline{T}\frac{\partial \overline{U}}{\partial x} dS \right) \tag{7}$$

where Γ is any path around the crack tip of the specimen, $\overline{T}$ is the surface traction, $\overline{W}$ is the strain energy density, $\overline{U}$ is the displacement vector and x, y are the Cartesian coordinates. The J-integral can be interpreted as the potential energy change with crack growth [2-4]. That is,

$$J = -\frac{1}{B}\frac{dU}{da} \tag{8}$$

where B is the thickness of the loaded body, a is the crack length and U is the total potential energy, which can be obtained by measuring the area under the load-displacement curve. Sumpter and Turner [32] later expanded the J-integral to consist of two components :

$$J = J_e + J_p \tag{9}$$

where J_e and J_p are the elastic and the plastic components of the total J value, respectively. Hence,

$$J_e = \frac{\eta_e U_e}{B(W-a)} \tag{10}$$

and

$$J_p = \frac{\eta_p U_p}{B(W-a)} \tag{11}$$

where U_e and U_p are the elastic and the plastic components of the total energy, η_e and η_p are their corresponding elastic and plastic work factors, $(W-a)$ is the ligament length and W is the width of the specimen. For a three-point SENB with a/W > 0.15, η_p is equal to 2. When the specimen has a span of 4W (S = 4W) and $0.4 < a/W < 0.6$, η_e is also equal to 2. Therefore, the Eq.(9) can be rewritten as:

$$J = \frac{2U}{B(W-a)} \tag{12}$$

ASTM E813 recommends Eq.(12) be used to calculate the J value for deeply notched SENB specimens.

4. ASTM E813-81 standard method

In the ASTM E813-81 standard method [21], the critical J value for crack initiation, J_{IC}, is determined by the intersection of the linear regression R-curve and the crack blunting line, $J = 2\sigma_y \Delta a$, σ_y is the uniaxial yield stress and Δa is the crack growth length. Two lines parallel to the crack blunting line at an offset of 0.6 W% (0.12 mm) and 6 W% (1.2 mm) are drawn as the minimum and the maximum exclusion lines, respectively.

The multiple-specimen technique is employed by loading the specimen to a controlled displacement and then unloading according to ASTM E813-81. The J value for each specimen at each controlled displacement is calculated by using Eq.(12). The linear regression R-curve intersects with the blunting line to locate the J_{IC} value as the critical fracture toughness.

5. ASTM E813-89 standard method

In the ASTM E813-89 standard method [22], the $J = C_1 \Delta a^{C_2}$ curve is fitted by a power law equation, , instead of a linear regression line. The critical J value, J_{IC}, is now at the intersection of the power law fitting line and the 0.2 mm offset line, i.e., $J = 2\sigma_y(\Delta\sigma - 0.2)$. This construction indicates that the J_{IC} value includes an additional 0.2 mm physical crack growth. Both the minimum and the maximum exclusion lines are parallel to the blunting line and offset at 0.15 and 1.5 mm, respectively. A good discussion of the ASTM E813-81 and ASTM E813-89 methods to evaluate the toughness of ductile polymer blends has been given by Mai and Powell [33].

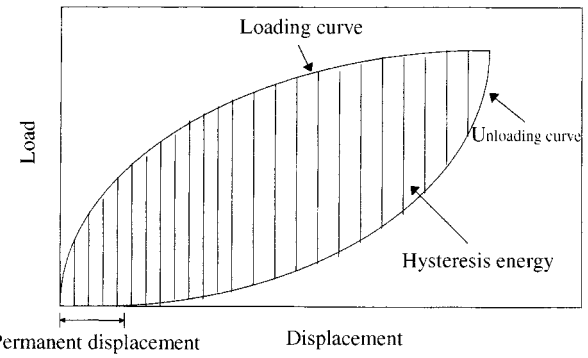

Figure 1. Definition of hysteresis energy in the loading-unloading versus displacement curve.

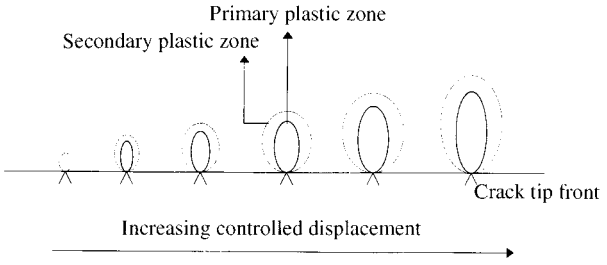

Figure 2. Schematic representation of the growth of the plastic zones.

6. J_{IC} validity requirements

For J_{IC} to be a valid fracture toughness, the specimen must meet certain size criteria to achieve a plane-strain stress state along the crack front. According to the ASTM E813 standard method [21, 22], these criteria are:

$$B,\ (W - a),\ W \geq 25(J_{IC}/\sigma_y) \tag{13}$$

Paris and co-workers [34] proposed the tearing modulus concept to describe the stability of a ductile crack in terms of elastic-plastic fracture mechanics. A non-dimensional parameter, tearing modulus T_m, has been defined by:

$$T_m = \frac{E}{\sigma_y^2}(dJ/da) \tag{14}$$

7. Hysteresis energy method

The hysteresis energy, defined as the energy difference between the loading and the unloading curves as shown in Figure 1, may include both crack blunting and crack extension. The energy density change during crack growth is given by:

$$-\frac{dU}{dA} = aW_o\{[\sum_{PL} G(x, y, \sigma_y)\,\delta_x\delta_y] - [\sum_{PU} G(x, y, \sigma_y)\,\delta_x\delta_y]\} \tag{15}$$

where PL and PU indicate the loading and unloading steps, respectively; W_o is the input energy density; G, g are functions of (x,y) and σ_y is the uniaxial yield stress. The quantity -dU/dA includes the energy available for forming the crack surface and the energy consumed in the plastic deformation of a cracked specimen. For a cracked specimen, there are three different regions around the crack tip, as shown in Figures 2(a) primary zone, 2(b) secondary zone and 2(c) fracture surface. When a pre-cracked specimen is being loaded before the onset of a crack extension (during crack blunting), a significant portion of the input energy is consumed and converted into a relatively large crack tip plastic zone for toughened polymeric materials. The specific energy balance equation for a cracked specimen can be described by the following equation:

$$\frac{1}{B}\frac{dU}{da} = \frac{1}{B}\left(\frac{dU_e}{da} + \frac{dU_k}{da} + \frac{dU_P^{PPZ}}{da} + \frac{dU_P^{SPZ}}{da}\right) + 2\gamma_s \tag{16}$$

The energy dissipated, defined as hysteresis energy (H), for a unit crack growth area of the system is given as follows:

$$\frac{dH}{dA} = \frac{1}{B}\left(\frac{dU_p^{ppz}}{da} + \frac{dU_p^{spz}}{da}\right) + 2\gamma_s \tag{17}$$

where U_k is kinetic energy, U_e is elastic energy, U_p^{ppz} is plastic energy for the primary zone, U_p^{spz} is plastic energy for the secondary zone and γ_s is fracture surface energy.

A specimen is loaded to a pre-determined displacement and then unloaded at the same rate by the multiple-specimen technique. The hysteresis energy (H) can be directly determined from the shaded area of the load-displacement curve as shown in Figure 1. In the PA6/PPE blends, the data window for the blunting line is experimentally set from 0 to 2 mm displacement, its corresponding crack extension being about 0.1 mm. The data beyond 2 mm displacement is fitted to a resistance line that accounts for many possible viscoelastic and inelastic energy dissipation micromechanisms, such as cavitation, debonding, crazing and shear yielding. The hysteresis energy will gradually increase with the increase of controlled displacement and the strain energy release due to crack growth will be included in the total hysteresis energy after crack extension. However, the rate of hysteresis energy increase is *substantially higher* than that resulting from the above mentioned pre-crack micromechanisms. Therefore, there exists a *clear transition* from crack

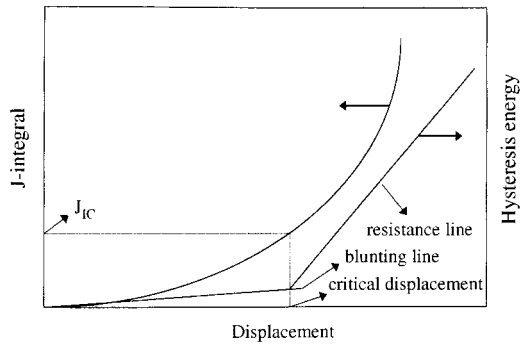

Figure 3. J-integral value obtained schematically by the hysteresis energy method.

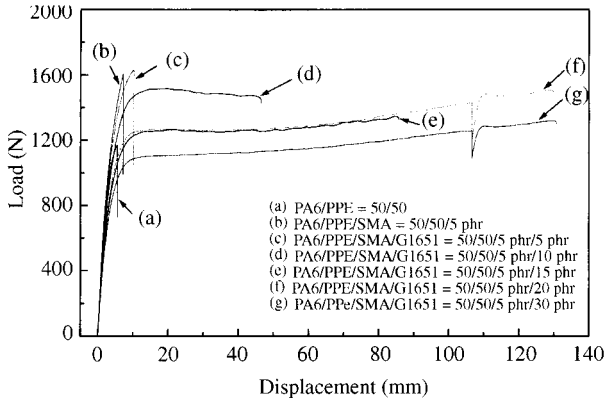

Figure 4. Curves of load versus displacement of PA6/PPE blends with various compositions in the standard tensile tests.

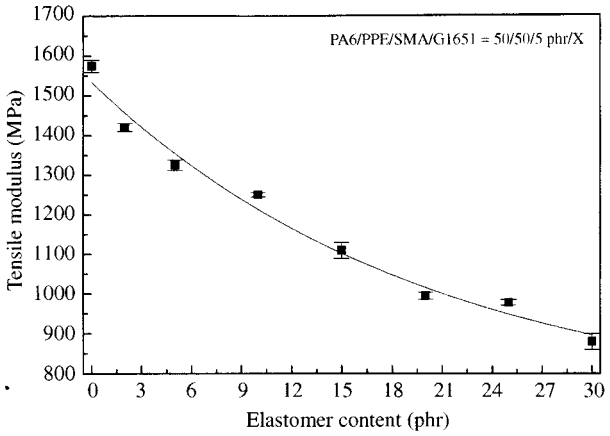

Figure 5. Effect of elastomer content upon the tensile modulus of PA6/PPE/SMA = 50/50/5 phr blend.

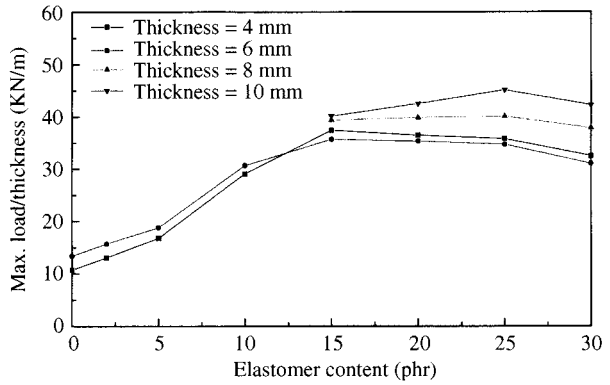

Figure 6. Effect of elastomer content upon maximum load per unit thickness of PA6/PPE/SMA = 50/50/5 phr blend.

blunting to crack extension that can be determined from the hysteresis energy-controlled displacement curve. Consequently, the critical displacement can be determined by these two linear lines and then the critical J-integral value, JIC, can be easily located in the J-integral-displacement curve as shown in Figure 3. The data observed to support this concept was reported in our previous papers [19,27-30].

Results and Discussion

1. Mechanical properties

For the standard tensile tests, the complete fracture load-displacement curves of the PA6/PPE blends are presented in Figure 4. The compatibilized blend has higher tensile strength than the uncompatibilized blend (curve (b) versus curve (a)). The yield stress of the compatibilized blend decreases with increasing elastomer content whereas the opposite trends for elongation and toughness are observed. Increasing elastomer content decreases the tensile modulus of the PA6/PPE/SMA (50/50/5 phr) blend, as shown in Figure 5. Data obtained from tensile tests according to ASTM D638 and dilatometry experiments are summarized in Table I. For the SENB specimens in the three-point bending tests, the effects of elastomer content on maximum load per unit thickness of the PA6/PPE/SMA (50/50/5 phr) blends is shown in Figure 6. The load-bearing capability of the blend increases with increasing elastomer content, and thicker specimens are superior to thinner ones. Figure 7 shows the effect of elastomer content on total fracture energy per unit thickness of PA6/PPE/SMA (50/50/5 phr) blend. Total fracture energy normally increases with increasing elastomer content but decreasing specimen thickness.

2. Critical stress intensity factor K_{IC}

Toughness data measured and analyzed according to ASTM D5045 are summarized in Table II. For blends with less than 10 phr elastomer, the valid K_{IC} values are relatively independent of specimen thickness (4 and 6 mm), but increase with increas-

Table I. Summary of tensile testing data of various compositions.

Composition	Tensile Stress (MPa)	Tensile Modulus (MPa)	Elongation (%)	Stress at Break (MPa)	Poisson ratio[a]
PA6/PPE=50/50	29.28±0.84	1458±28	9.28±0.33	29.28±0.84	0.42
PA6/PPE/SMA=50/50/5 phr	38.31±0.93	1574±15	12.81±0.80	38.31±0.93	0.41
PA6/PPE/SMA/G1651=50/50/5 phr/2 phr	42.35±1.04	1421±10	19.45±1.00	42.35±1.04	-----
PA6/PPE/SMA/G1651=50/50/5 phr/5 phr	40.27±0.37	1326±13	23.90±1.50	40.23±0.37	0.40
PA6/PPE/SMA/G1651=50/50/5 phr/10 phr	38.19±0.74	1251±5	95.24±2.00	37.12±0.52	0.43
PA6/PPE/SMA/G1651=50/50/5 phr/15 phr	34.22±1.00	1111±20	194.79±3.00	33.99±0.90	0.41
PA6/PPE/SMA/G1651=50/50/5 phr/20 phr	31.96±0.95	996±9	259.69±3.21	37.88±1.20	0.41
PA6/PPE/SMA/G1651=50/50/5 phr/25 phr	29.61±0.85	979±7	213.33±4.20	33.36±0.78	-----
PA6/PPE/SMA/G1651=50/50/5 phr/30 phr	28.28±0.90	880±20	261.47±2.50	33.11±0.89	0.41

(a) Value obtained from tensile dilatometry tests.

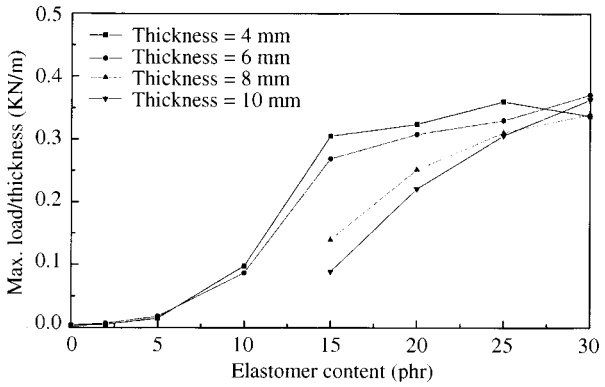

Figure 7. Effect of elastomer content upon total fracture energy per unit thickness of PA6/PPE/SMA = 50/50/5 phr blend.

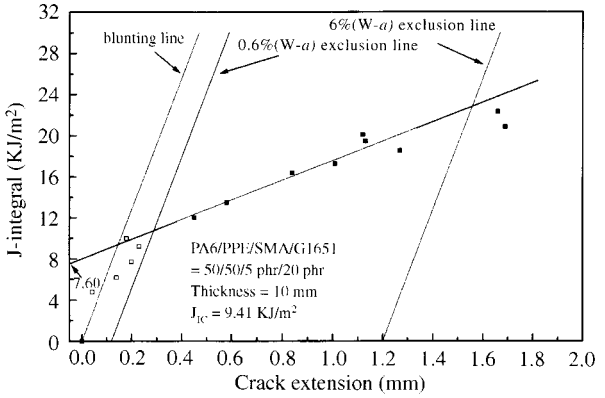

Figure 8. J-integral curves obtained by the ASTM E813-81 and the modified ASTM E813-81 methods for the PA6/PPE/SMA/G1651 = 50/50/5 phr/20 phr blend.

ing elastomer content at a given specimen thickness. Their fracture behavior is in the plane-strain state and can be described by LEFM. For blends with more than 10 phr elastomer, the yield stress decreases quite sharply so that plane-strain fracture is difficult to maintain even in the 10 mm thick specimens. Therefore, these fracture toughness is in plane-strain or in mixed mode.

3. J-integral analysis by ASTM standards and their modified methods

Figure 8 plots the acceptable J versus data Δa according to ASTM E813-81 and its modified version for PA6/PPE/SMA/G1651 (50/50/5 phr/20 phr) blend with a thickness of 10 mm. The linear regression R-curve intersects with the blunting line to give the critical J value, J_{IC} = 9.41 KJ/m^2. Also, another critical J value, J_{IC} = 7.60 KJ/m^2, can be obtained from the intersection of the linear regression R-curve with the y-axis at Δa = 0, as suggested by Narisawa [11]. This modified method neglects the occurrence of crack tip blunting and yields a much more conservative value for some materials [7,11,33,35].

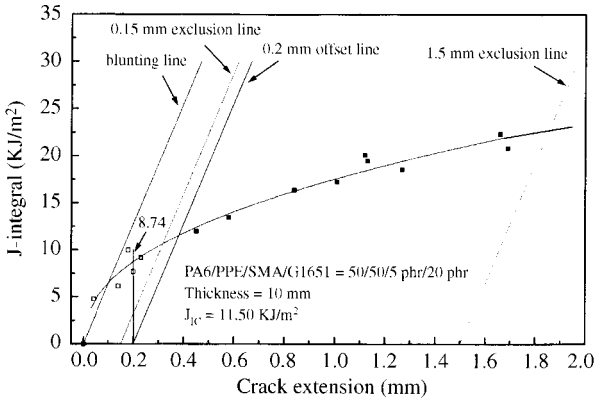

Figure 9. J-integral curves obtained by the ASTM E813-89 and the modified ASTM E813-89 methods for the PA6/PPE/SMA/G1651 = 50/50/5 phr/20 phr blend.

Plots of the acceptable J versus Δa data according to ASTM E813-89 and its modification for the same blend with the thickness of 10 mm are given in Figure 9. The critical value, J_{IC} = 11.50 KJ/m^2, is determined by the intersection of the power-law re-

Table II. Summary of K_{IC} (or K_{IQ}) and G_{IC} (G_{IQ}) data.

Composition	Thickness (mm)	K_{IQ} or K_{IC} (MPa × $m^{1/2}$)	G_{IQ} or G_{IC}[(a)] (KJ/m^2)	Plane strain	Yielding
PA6/PPE = 50/50	4	1.30±0.10	0.96±0.09	Y	N
PA6/PPE/SMA = 50/50/5 phr	4	0.95±0.09	0.48±0.12	Y	N
PA6/PPE/SMA/G1651 = 50/50/5 phr/2 phr	4	1.16±0.02	0.79±0.07	Y	N
PA6/PPE/SMA/G1651 = 50/50/5 phr/5 phr	4	1.45±0.04	1.32±0.10	Y	Y
PA6/PPE/SMA/G1651 = 50/50/5 phr/10 phr	4	2.22±0.06	3.28±0.08	N	Y
PA6/PPE/SMA/G1651 = 50/50/5 phr/15 phr	4	2.66±0.11	5.30±0.12	N	Y
PA6/PPE/SMA/G1651 = 50/50/5 phr/20 phr	4	2.67±0.07	5.95±0.15	N	Y
PA6/PPE/SMA/G1651 = 50/50/5 phr/25 phr	4	2.48±0.03	5.24±0.04	N	Y
PA6/PPE/SMA/G1651 = 50/50/5 phr/30 phr	4	2.22±0.06	4.66±0.07	N	Y
PA6/PPE = 50/50	6	1.47±0.14	1.23±0.12	Y	N
PA6/PPE/SMA = 50/50/5 phr	6	1.19±0.08	0.75±0.20	Y	N
PA6/PPE/SMA/G1651 = 50/50/5 phr/2 phr	6	1.39±0.04	1.13±0.10	Y	N
PA6/PPE/SMA/G1651 = 50/50/5 phr/5 phr	6	1.67±0.07	1.75±0.09	Y	Y
PA6/PPE/SMA/G1651 = 50/50/5 phr/10 phr	6	2.44±0.10	3.96±0.07	N	Y
PA6/PPE/SMA/G1651 = 50/50/5 phr/15 phr	6	2.40±0.08	4.31±0.02	N	Y
PA6/PPE/SMA/G1651 = 50/50/5 phr/20 phr	6	2.34±0.06	4.57±0.12	N	Y
PA6/PPE/SMA/G1651 = 50/50/5 phr/25 phr	6	2.25±0.05	4.32±0.04	N	Y
PA6/PPE/SMA/G1651 = 50/50/5 phr/30 phr	6	2.15±0.04	4.37±0.06	N	Y
PA6/PPE/SMA/G1651 = 50/50/5 phr/15 phr	8	3.08±0.06	6.31±0.15	N	Y
PA6/PPE/SMA/G1651 = 50/50/5 phr/20 phr	8	2.85±0.09	6.08±0.09	N	Y
PA6/PPE/SMA/G1651 = 50/50/5 phr/25 phr	8	2.63±0.05	5.90±0.07	N	Y
PA6/PPE/SMA/G1651 = 50/50/5 phr/30 phr	8	2.43±0.02	5.58±0.06	N	Y
PA6/PPE/SMA/G1651 = 50/50/5 phr/15 phr	10	3.03±0.07	6.11±0.20	N	Y
PA6/PPE/SMA/G1651 = 50/50/5 phr/20 phr	10	2.87±0.05	6.17±0.10	N	Y
PA6/PPE/SMA/G1651 = 50/50/5 phr/25 phr	10	3.11±0.10	8.24±0.08	N	Y
PA6/PPE/SMA/G1651 = 50/50/5 phr/30 phr	10	2.65±0.06	6.64±0.17	N	Y

(a) $G_{IC} = K_{IC}^2/E\ (1 - \nu^2)$

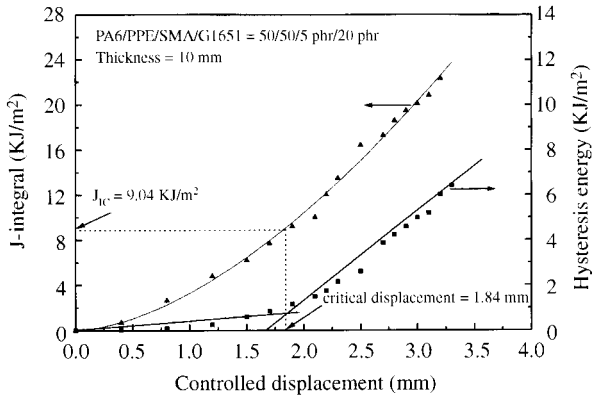

Figure 10. J-integral value obtained by the hysteresis energy method for the PA6/PPE/SMA/G1651 = 50/50/5 phr/20 phr blend.

gression line with the 0.2 mm offset line. Pandey, Sundaram and Kumar [36] utilized various methods for the evaluation of J-initiation toughness on Mo and Cr-Mo steel at different temperatures by the SENB configuration. They adopted the intersection of the R-curve with the 0.2 mm physical crack growth instead of the 0.2 mm offset blunting line to determine J_{IC}. They also recommended locating J_{IC} at the intersection of the R-curve with the vertical line corresponding to the stretch zone width (SZW) as measured on the specimen. Therefore, from the modified ASTM E813-89 method, a vertical 0.2 mm offset line is adopted to determine the critical J value, J_{IC} = 8.74 KJ/m^2. The critical J-integral values of the blends with different elastomer contents and with different thicknesses determined by various methods are summarized in Table III.

4. Hysteresis energy method

Figure 10 shows J versus Δa data according to the hysteresis energy method for the 10 mm thick PA6/PPE/SMA/G1651 (50/50/5 phr/20 phr) blends. The critical displacement, D_{IC} = 1.84 mm , is located at the intersection of the crack blunting line and the crack growth resistance line. As soon as the critical displacement is identified, the corresponding critical J value, J_{IC} = 9.04 KJ/m^2, is then determined from the J-integral versus the controlled displacement curve. The critical J-integral values of the blends with various elastomer contents and different thicknesses determined by the hysteresis en-

Table III. Summary of J_{IC} determined by different methods (Unit : KJ/m^2).

Composition Thickness method	ASTM E813-81	Modified ASTM E813-81	ASTM E813-89	Modified ASTM E813-89	Hysteresis energy
PA6/PPE/SMA/G1651 = 50/50/5 phr/10 phr					
4 mm	1.27±0.02	0.79±0.02	3.24±0.12	2.84±0.16	2.95±0.12
6 mm	3.64±0.08	3.31±0.08	3.94±0.15	3.65±0.20	2.82±0.16
PA6/PPE/SMA/G1651 = 50/50/5 phr/15 phr					
4 mm	8.77±0.12*	6.50±0.12*	11.00±0.20*	7.66±0.12*	7.66±0.09*
6 mm	9.67±0.16*	7.47±0.16	11.38±0.25*	8.19±0.21	7.66±0.15
8 mm	7.28±0.20	6.50±0.20	8.08±0.12	6.92±0.17	6.86±0.21
10 mm	5.85±0.18	5.27±0.18	6.75±0.23	5.68±0.25	6.93±0.17
PA6/PPE/SMA/G1651 = 50/50/5 phr/20 phr					
4 mm	12.85±0.26*	9.86±0.26*	14.63±0.18*	10.07±0.27*	8.88±0.15*
6 mm	7.89±0.24*	5.20±0.24	11.11±0.20*	7.22±0.31	9.42±0.10*
8 mm	11.23±0.02*	9.28±0.02	12.75±0.25*	9.65±0.18	9.40±0.20
10 mm	9.41±0.15	7.60±0.15	11.50±0.13	8.74±0.23	9.04±0.18
PA6/PPE/SMA/G1651 = 50/50/5 phr/25 phr					
4 mm	10.97±0.16*	7.41±0.16*	14.63±0.25*	8.94±0.19*	9.03±0.21*
6 mm	9.67±0.24*	6.24±0.25	13.00±0.27*	7.81±0.25*	8.87±0.23*
8 mm	11.16±0.18*	7.73±0.18	14.63±0.18*	9.23±0.14	9.37±0.15
10 mm	11.60±0.02*	8.18±0.02	15.38±0.30*	9.68±0.21	10.17±0.18
PA6/PPE/SMA/G1651 = 50/50/5 phr/30 phr					
4 mm	7.53±0.28*	4.10±0.28	12.88±0.17*	7.38±0.17*	8.90±0.15*
6 mm	12.92±0.15*	8.91±0.15*	15.57±0.32*	9.24±0.23*	9.55±0.24*
8 mm	12.71±0.12*	8.64±0.12	17.00±0.26*	10.35±0.30*	9.83±0.17*
10 mm	12.19±0.20*	7.46±0.20	16.83±0.27*	9.33±0.21	10.29±0.12*

Modified ASTM E813-81: extrapolate the R-curve least square line to $\Delta a = 0$ and obtain the J_{IC} value.
Modified ASTM E813-89: use a vertical line with 0.2 mm offset as the offset line.
*, size requirements (i.e., Eq.(13)) not met.

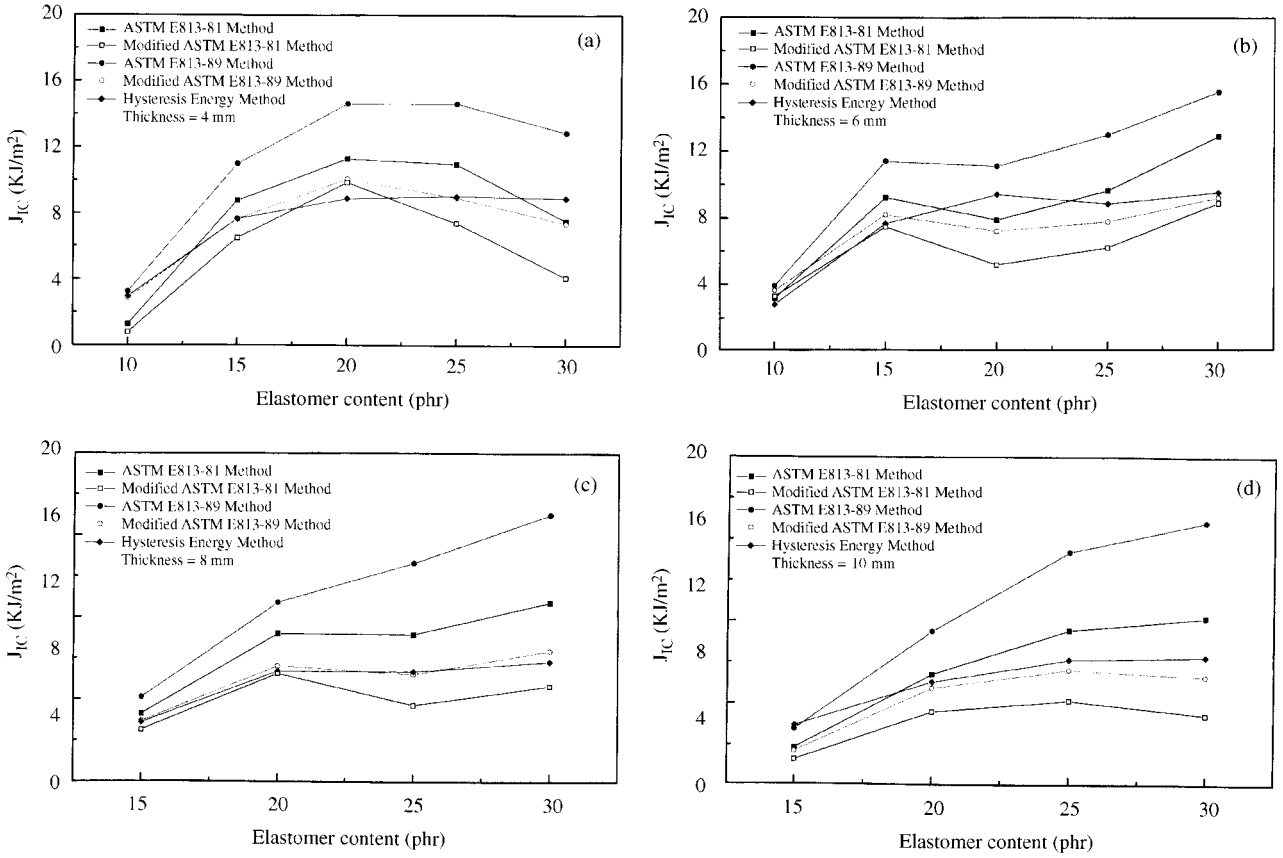

Figure 11. Effect of elastomer content upon J-integral values determined by various methods at different thickness (a) 4 mm, (b) 6 mm, (c) 8 mm and (d) 10 mm.

Table IV. Summary of tearing moduli and size criterion according to ASTM E813-89 method for various compositions.

Composition	Thickness (mm)	dJ_R/da (MJ/m^3)	Tearing modulus (T_m)[(a)]
PA6/PPE/SMA/G1651 = 50/50/5 phr/10 phr	4	4.3	3.7
PA6/PPE/SMA/G1651 = 50/50/5 phr/15 phr	4	11.9	11.3
PA6/PPE/SMA/G1651 = 50/50/5 phr/20 phr	4	11.3	11.0
PA6/PPE/SMA/G1651 = 50/50/5 phr/25 phr	4	13.4	15.0
PA6/PPE/SMA/G1651 = 50/50/5 phr/30 phr	4	18.1	20.0
PA6/PPE/SMA/G1651 = 50/50/5 phr/10 phr	6	3.2	2.7
PA6/PPE/SMA/G1651 = 50/50/5 phr/15 phr	6	10.0	9.5
PA6/PPE/SMA/G1651 = 50/50/5 phr/20 phr	6	13.9	13.5
PA6/PPE/SMA/G1651 = 50/50/5 phr/25 phr	6	16.3	18.2
PA6/PPE/SMA/G1651 = 50/50/5 phr/30 phr	6	12.5	13.8
PA6/PPE/SMA/G1651 = 50/50/5 phr/15 phr	8	4.9	4.6
PA6/PPE/SMA/G1651 = 50/50/5 phr/20 phr	8	6.3	6.1
PA6/PPE/SMA/G1651 = 50/50/5 phr/25 phr	8	12.2	13.6
PA6/PPE/SMA/G1651 = 50/50/5 phr/30 phr	8	13.1	14.4
PA6/PPE/SMA/G1651 = 50/50/5 phr/15 phr	10	7.3	6.9
PA6/PPE/SMA/G1651 = 50/50/5 phr/20 phr	10	6.9	6.7
PA6/PPE/SMA/G1651 = 50/50/5 phr/25 phr	10	13.8	15.4
PA6/PPE/SMA/G1651 = 50/50/5 phr/30 phr	10	16.7	18.3

(*a*) $T_m = E/\sigma_y^2 (dJ/da)$

ergy method are summarized in Table III.

5. Effect of elastomer content and thickness upon J_{IC} determined by various methods

Figures 11(a)-11(d) show the effect of elastomer content on the J_{IC} values determined by various methods using different specimen thicknesses. In general, J_{IC} increases with increasing elastomer content at the same thickness. J_{IC} from ASTM E813-89 is always the highest since it includes an additional 0.2 mm crack extension. J_{IC} from modified ASTM E813-81 is always the lowest since it does not consider crack blunting. Compared to J_{IC} values obtained from ASTM E813-81, these J_{IC} values are 11-71% higher from ASTM E813-89, 3-24% lower from modified ASTM E813-89, 4-31% lower from the hysteresis energy method and 10-46% lower from modified ASTM E813-81. Therefore, the JIC values based on ASTM E813-81, modified ASTM E813-89 and the hysteresis energy methods are comparable to one another. Indeed, J_{IC} values from the hysteresis energy method and modified ASTM E813-89 are substantially close to each other. The advantage of these two methods results in J_{IC} quite independent of specimen thickness, counting only those values that have satisfied the size requirements of Eq. (13), Table III. However, the physical reason leading to thickness-invariant toughness is not clear at this stage. In this case, these two methods are considered most appropriate to determine the fracture toughness of this G1651-toughened PA6/PPE/SMA blending system.

While J_{IC} gives the toughness at tear initiation, the entire R-curve provides the resistance to crack propagation. The slope of the R-curve at a given extent of crack extension is indicative of the relative stability of crack growth. The shape of the R-curve depends upon material behavior and, to a lesser extent, upon the configuration of the cracked structure. The slope of the R-curve gradually becomes steeper with increasing elastomer content and decreasing thickness in these toughened PA6/PPE/SMA blends. The slope of the R-curve is usually quantified by a non-dimensional parameter, tearing modulus T_m defined by Eq.(14). The tearing moduli of the blends with various compositions and different thicknesses are listed in Table IV. T_m increases with increasing elastomer content. A higher tearing modulus implies that a specimen is able to sustain more stable crack growth for the same test geometry. Hence, blends with larger amounts of elastomer will have improved fracture toughness against tear propagation.

Conclusions

The fracture toughness of the blend, brittle or with small-scale yielding, can be well described by the critical stress intensity factor, K_{IC}, and the strain energy release rate, G_{IC}. Under the plane-strain condition, K_{IC} and G_{IC} are independent of thickness

and increase with increasing elastomer content.

For ductile blends, several methods are utilized to evaluate the critical J-integral, J_{IC}, which increases generally with increasing elastomer content. Also, the slope of the R-curve becomes steeper with increasing elastomer content and decreasing specimen thickness. J_{IC} values determined from ASTM E813-89 are always the highest since they are overestimated by including an additional 0.2 mm physical crack growth. J_{IC} values determined from modified ASTM E813-81 are always the lowest because they are underestimated by not including the occurrence of crack tip blunting. J_{IC} values determined from the two methods, modified ASTM E813-89 and hysteresis energy, are compared to and can be utilized to characterize tear initiation toughness of the compatibilized PA6/PPE blends. These J_{IC} values appear to be invariant with specimen thickness and they are acceptable as potential alternative techniques to evaluate the critical J-integral for toughened polymer blends.

Acknowledgement

The financial support of the scholarship from the Ministry of Education, Taiwan, Republic of China, to one of authors (K. C. Chiou) is greatly appreciated. Y. W. Mai is supported by the Australian Research Council for his work on toughening mechanisms and mechanics of polymer blends.

References

1. C. B. Bucknall, *Toughened Plastics*, Applied Science Publishers, London (1977).
2. J. R. Rice, *J. Appl. Mech.*, **35**, 379 (1968) .
3. J. A. Begley and J. D. Landes, *ASTM STP*, **514**, 1 (1972).
4. J. D. Landes and J. A. Begley, *ASTM STP*, **560**, 170 (1974).
5. M. K. V. Chan and J. G. Williams, *Int. J. Fract.*, **19**, 145 (1983).
6. S. Hashemi and J. G. Williams, *Polymer*, **27**, 384 (1986).
7. D. D. Huang and J. G. Williams, *J. Mater. Sci.*, **22**, 2503 (1987).
8. P. K. So and L. J. Broutman, *Polym. Eng. Sci.*, **26**, 1173 (1986).
9. E. J. Moskala and M. R. Tant, *Polym. Mater. Sci. Eng.*, **63**, 63 (1990).
10. C. M. Rimnac, T. M. Wright and R. W. Klein, *Polym. Eng. Sci.*, **28**, 1586 (1988).
11. I. Narisawa, *Polym. Eng. Sci.*, **27**, 41 (1987).
12. I. C. Tung, *Polym. Bull.*, **25**, 253 (1991).
13. R. K. Singh and K. S. Parihar, *J. Mater. Sci.*, **21**, 3921 (1986).
14. S. Hashemi and J. G. Williams, *J. Mater. Sci.* **26**, 621 (1991).
15. E. J. Moskala, *J. Mater. Sci.*, **27**, 4483 (1992).
16. J. Wu, Y. W. Mai, and B. Cotterell, *J. Mater. Sci.*, **28**, 3373 (1993).
17. T. Yuhara and M. T. Kortschot, *J. Mater. Sci.*, **28**, 3571 (1993).
18. B. A. Crouch and D. D. Huang, *J. Mater. Sci.*, **29**, 861 (1994).
19. M. L. Lu and F. C. Chang, *Polymer*, **36**, 2541 (1995).
20. J. R. Rice, P. C. Pairs and J. G. Merkle, *ASTM STP*, **536**, 231 (1973).
21. ASTM Standard E813-81 in *Annual Book of ASTM Standards*, **03.01**, ASTM, Philadelphia, PA, 810 (1981).
22. ASTM Standard E813-89 in *Annual Book of ASTM Standards*, **03.01**, ASTM, Philadelphia, PA, 700 (1989).
23. Y. W. Mai and B. Cotterell, *Eng. Fract. Mech.*, **21**, 123 (1985).
24. W. N. Chung and J. G. Williams, *ASTM STP*, **1114**, 320 (1991).
25. S. Seidler and W. Grellmnn, *J. Mater. Sci.*, **28**, 4078 (1993).
26. Z. Zhou, J. D. Landes and D. D. Huang, *Polym. Eng. Sci.*, **34**, 128 (1994).
27. B. C. Lee, M. L. Lu, and F. C. Chang, *J. Appl. Polym. Sci.*, **47**, 1867 (1993).
28. M. L. Lu, K. C. Chiou and F. C. Chang, *Polym. Eng. Sci.*, **36**, 2289 (1996).
29. M. L. Lu, K. C. Chiou and F. C. Chang, *J. Appl. Polym. Sci.*, **62**, 863 (1996).
30. M. L. Lu, K. C. Chiou and F. C. Chang, *J. Polym. Res.*, **3**, 73 (1996).
31. K. C. Chiou and F. C. Chang, *J. Appl. Polym. Sci.*, Accepted.
32. J. D. Sumpter and C. E. Turner, *Int. J. Fract.*, **9**, 320 (1973).
33. Y. W. Mai and P. Powell, *J. Polym. Sci., Polym.* Phys., **29**, 785 (1991).
34. P. C. Paris, H. Tada, A. Zahoor and H. Ernst, *ASTM STP*, **668**, 5 (1979).
35. I. Narisawa and M. T. Takemori, *Polym. Eng. Sci.*, **29**, 671 (1989).
36. R. K. Pandey, P. Sundaram and A. N. Kumar, *J. Testing Evaluation*, **20**, 106 (1992).